International Journal of Theoretical & Applied Computational Intelligence
https://ijtaci.com

Research Article

White Blood Cells Classification Based on a New Strategy to Cluster Channels RGB of Blood Smear Image Using Resnet-18 Model

Amenah Y. Abdzaid[1], Dheia N. Khadum[2], Saad Salah Al-Barrak[2], Aymen Saad[3,4*]

[1] Fatima Al Zahra School for Distinguish Students, AL-Diwaniyah Education Directorate, Iraq
[2] Medical Instruments Techniques Dept. Babylon Technical Institute Al-Furat Al-Awsat Technical University, Iraq
[3] Higher Institute of Nanotechnology for Graduate Studies, Al-Furat Al-Awsat Technical University, Najaf, Iraq
[4] School of Electrical Engineering, Universiti Teknologi Malaysia, Skudai, Johor, Malaysia.

*Corresponding author: aymen.abdalameer@atu.edu.iq

https://orcid.org/0000-0002-3582-6799

Received: 18/02/2026; Accepted: 22/03/2026; Published: 07/04/2026

https://doi.org/10.65278/IJTACI.2026.64

Abstract- White Blood Cells (WBCs) play a critical role in the human immune system, and their accurate identification is essential for diagnosing many hematological diseases. Manual analysis of blood smear images (BSI) under a microscope is time-consuming and prone to human error. Recently, deep learning techniques have demonstrated strong capabilities in automated medical image classification. This paper proposes a novel strategy to improve WBC classification by clustering the RGB channels of blood smear images to generate an augmented dataset, which is subsequently used to train a ResNet-18 deep learning model. In the proposed approach, image preprocessing techniques, including morphological operations and RGB channel clustering, are applied to enhance image quality and create additional training samples. The dataset consists of four WBC classes: eosinophils, lymphocytes, monocytes, and neutrophils. Two experiments were conducted to evaluate the effectiveness of the proposed method. The first experiment used the original dataset, while the second experiment used the augmented dataset produced through RGB channel clustering. Experimental results show that the proposed strategy significantly improves classification performance, increasing the overall accuracy from approximately 86.89% and 99.17%. These findings demonstrate that the proposed preprocessing and augmentation approach enhances feature representation and improves the effectiveness of deep learning models for automated WBC classification.

Keywords: White blood cells (WBC), blood smear images (BSI), Deep Learning (DL), classification

1. Introduction

Leukaemia or White Blood Cells (WBCs) Leukocytes are crucial to the body's defence against sickness even though they are much less abundant than red blood cells [1]. WBCs range in density from 4000 to 11.000/mm3 and make up less than 1.0% of the entire blood volume [2]. The only fully developed blood cells, or those with nuclei and the typical organelles, are white blood cells [3]. The moveable army of leukocytes acts as a barrier between the body and harmful germs, viruses, parasites, and tumour cells. They possess some unique qualities as a result. Red blood cells only exist in the bloodstream and carry out their tasks there [4]. Contrarily, white blood cells can enter and exit blood arteries [5]. Simply put, they are transported by the circulatory system to the parts of the body where they are required for immunological or inflammatory reactions. During positive chemotaxis, leukocytes reaction to damaged cells aids in identifying the infected tissues [6]. Once the WBCs have created the cytoplasmic extensions, they begin to move in an undefined manner all through the tissue gaps [7]. They locate areas of tissue injury by following the diffusion gradient, and then they swarm to eliminate dead cells or bacteria in huge numbers. Whenever the functions of WBCs arise, the body rapidly produces a high number WBCs which may be twice the normal threshold. These high populations of WBCs are transported to the systemic circulation within a few hours [8].

The aim of this study is to develop a novel strategy for classifying white blood cells by effectively clustering the RGB channels of blood smear images using the ResNet-18 model. This approach seeks to enhance the accuracy and efficiency of white blood cell classification, ultimately contributing to improved diagnostic capabilities in hematology. The research will explore the integration of advanced image processing techniques with deep learning to optimize the identification and categorization of various white blood cell types.

2. Types of WBCS:

The two groups of leucocytes are categorised based on the granules present or absent in their cytoplasm given in Figure 1 [9].

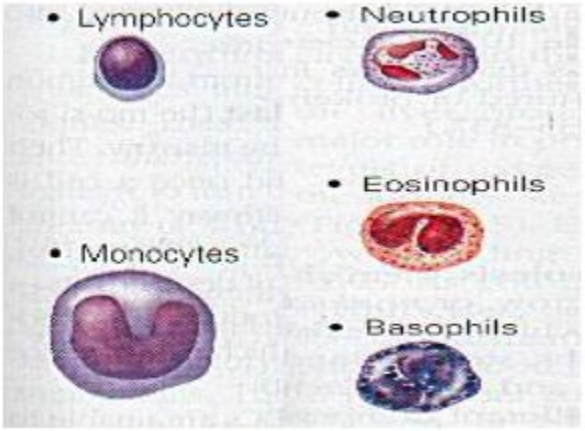

Figure 1: Microscopic views of WBCs. Granulocyte types

2.1 Granulocyte types:

2.1.1 Neutrophils

Have Very Small Granules With A Multiplied Nucleus (3-5 Lobes) That React To Both Basic And Acid Stains. As A Result, The Entire Cytoplasm Shows Pink Staining. At The Sites Of Acute Infection, Neutrophils Are Active Phagocytes [10].

2.1.2 Eosinophils

Are Granulocytes With A Bilobed Nucleus, Blue Cytoplasm And Orange To Red Cytoplasmic Granules. ItS Shape Is Like An Ancient Telephone With Large Cytoplasmic Granules With A Red Colouration. The Populations Of Eosinophils Are Remarkably Increased During Parasitic Infestations And Infections., As Well As Allergic Reactions [11].

2.1.3 Basophils

Are The Most Uncommon Leucocytes. The Histamine Present In Their CytOplasmIc Granules Has A Strong Affinity For Basic Dyes And Appears Purplish-Black When StainEd. Histamine Is An Inflammatory Substance With Vasodilating PropertIes, Thereby Attracting Other Wbcs To The Site Of Inflammation. The Effects Of Histamine Are Antagonized By Medications Known As Antihistamines. Upon Staining, Either A U Or S-Shaped Deep Purple Core Characterised By Single Or Double Pronounced Restrictions Is Visualised [12].

2.1.4 Agranulocytes

Have No Distinct Granules In Their Cytoplasm Possess And Their Nuclei Are Either Oval Or Kidney-Shaped. The Two Types Of Agranulocytes In Mammals Are monocytes And Lymphocytes.

- Lymphocytes are generally characterised by a large dark purple colour. RBCs are slightly smaller than lymphocytes. The latter are located in the lymphatic tissues, where they play active roles in the immune response. The two types of lymphocytes are:
  * T lymphocytes: responsible for cell-mediated immunity.
  * B lymphocytes: responsible for humoral immunity [13].
- Monocyte are immune cells comprising chemoreceptors and pathogen recognition receptors that are either found in the systemic circulation or localized in lymphoid tissues. They are similar to lymphocytes apart from their large cytoplasm and kidney-like nucleus. Monocytes are transformed into connective tissues during migration. Meanwhile, chronic infections such as tuberculosis could be attacked by macrophages. Granulocytes and monocytes protect the body from foreign organisms by engulfing them via phagocytosis. Lymphocytes depend on the immune system to function properly. Nevertheless, like the granulocytes and monocytes, some lymphocytes bind and destroy specific foreign bodies [14].

Concentrations of the Different White Blood Cells in the Blood: There is approximately 11000 WBCs/mm3 volume of blood in an adult human being. The normal proportion of WBCs is approximately 62.0% for neutrophils, 30.3% for lymphocytes, 5.3% for monocytes, 2.3% and eosinophils and 0.4% for Basophils [15].

Despite the significant progress achieved in automated WBC classification, several challenges remain. Traditional microscopic examination relies heavily on manual observation by medical experts, which is time-consuming and susceptible to human error and subjectivity. In addition, many conventional image processing approaches depend on handcrafted feature extraction techniques that may fail to capture complex morphological and color characteristics of blood cells. These limitations often lead to reduced classification accuracy, especially when dealing with variations in staining conditions, illumination, and

cell morphology. Although deep learning approaches have improved classification performance, their effectiveness is often limited by insufficient feature representation and the availability of large, diverse training datasets.

To address these challenges, this paper proposes a novel strategy to enhance white blood cell classification by clustering the RGB channels of blood smear images to generate an augmented dataset. The augmented dataset is then used to train a ResNet-18 deep learning model through transfer learning. The proposed approach aims to improve feature representation and classification performance by combining image enhancement techniques, morphological processing, and RGB channel clustering. The main contribution of this study is the development of a preprocessing framework that increases the effective dataset size and enhances the discriminative features of WBC images, resulting in a significant improvement in classification accuracy compared with the use of the original dataset alone.

3. Materials and Methods

The methodology adopted in this paper consists of four main steps: data downloading, preprocessing, feature extraction, and dataset classification. Figure 2 illustrates these phases in detail. The proposed CNN-based skin image classification framework is implemented using MATLAB 2021a. The experiments are conducted on a system with the following specifications: Windows 10 operating system, 8 GB DDR4 RAM, AMD Ryzen 5 3550H CPU, and Radeon Vega Mobile GFX (2.10 GHz).

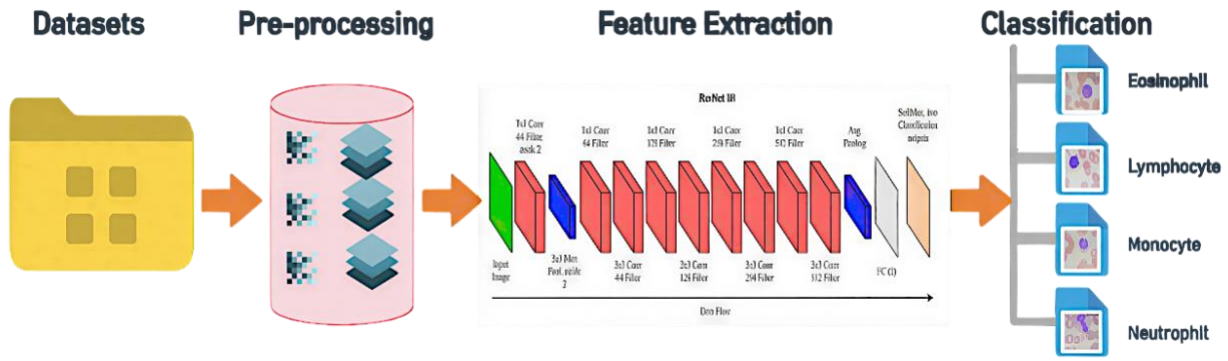

Figure 2: Overview of the proposed methodology

3.1 Dataset

The blood smear image dataset was obtained from Kaggle [16]. It consists of four classes: Eosinophil, Lymphocyte, Monocyte, and Neutrophil. Each folder contains 3,091 samples, and the total of samples is 12,364. In addition, the classes have the same number of images to avoid biased results.

3.2 Dataset Preparation

The dataset is split into training and testing sets, with 80% of the images used for training the algorithm and 20% reserved for validation. The training process is conducted at three levels to minimize computational resource consumption.

3.3 Resnet-18

ResNet-18 is a convolutional neural network introduced by He et al. in the original Residual Network (ResNet) paper. It is composed of an initial convolutional layer, followed by four stages of residual blocks,

and ends with global average pooling and a fully connected classification layer. The key idea of ResNet is the use of residual connections, also called skip connections, which allow the input of a block to be added directly to its output. This helps the network learn a residual mapping instead of a complete transformation, making optimization easier and reducing the degradation problem that occurs when deeper networks are trained. In ResNet-18, each residual block typically contains two convolutional layers with batch normalization and ReLU activation. When the input and output dimensions are the same, the identity mapping is added directly. When dimensions differ, a projection shortcut is used to match them. This architecture enables efficient gradient flow during backpropagation and has been widely adopted in image classification tasks because of its good balance between accuracy and computational complexity [17].

For this study, ResNet-18 was selected because it is a lightweight and effective deep learning model suitable for medical image classification, especially when combined with transfer learning given in Figure 3. Its residual learning mechanism allows it to capture discriminative features from WBC images while maintaining relatively low computational cost.

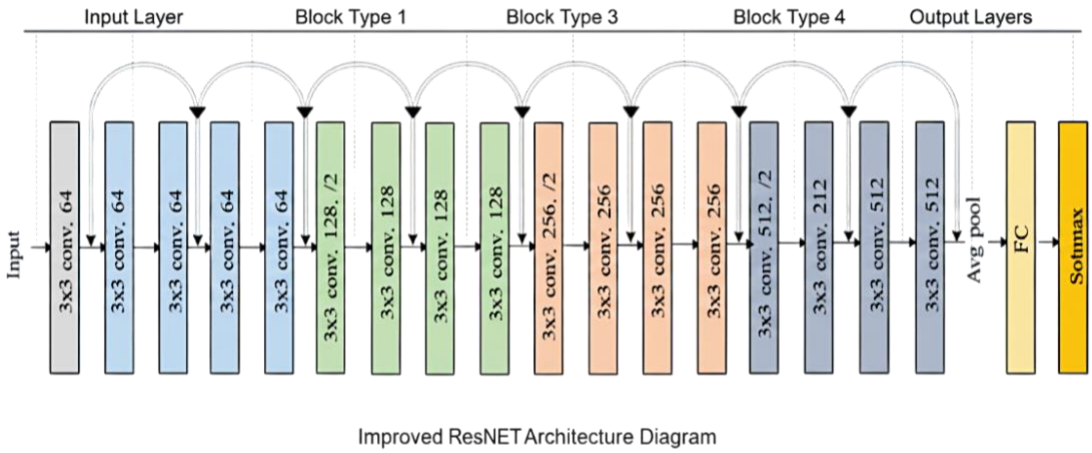

Figure 3: ResNet-18 structure.

3.4 Analysis Of Wb Images

In order to get around the drawbacks of feature extraction and high resolution, we offer enough datasets in this study. We conducted two tests to do that:

1. In the first experiment, the CNN suggested model is used to realize all datasets from their initial size to 224×224×3. Then, 20% and 80% of each dataset class are separated for testing and training data, respectively. Finally, the training dataset is fed into the ResNet-18 model for training, as illustrated in Figure 4.

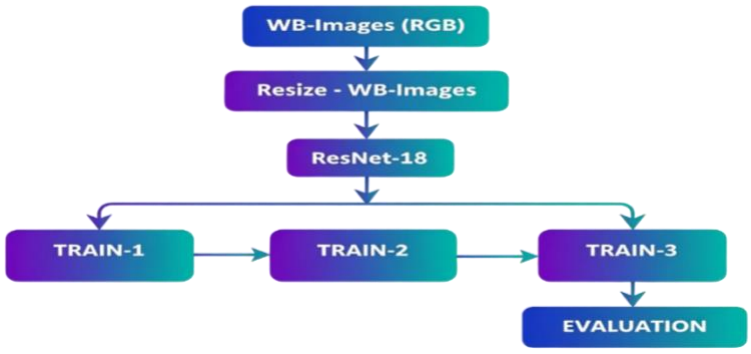

Figure 4: experiment (1) - Training ResNet-18 on the original dataset.

2. Image enhancement techniques are introduced in the second experiment on the same images presented previously, which are represented by morphological structuring and clustering channels RGB, and then a new dataset is acquired as depicted in Figure 5. The new dataset consists of triple the number of the original dataset, thus having a total number of 9273 images in each class. Overall, a total of 37,092 images are obtained.

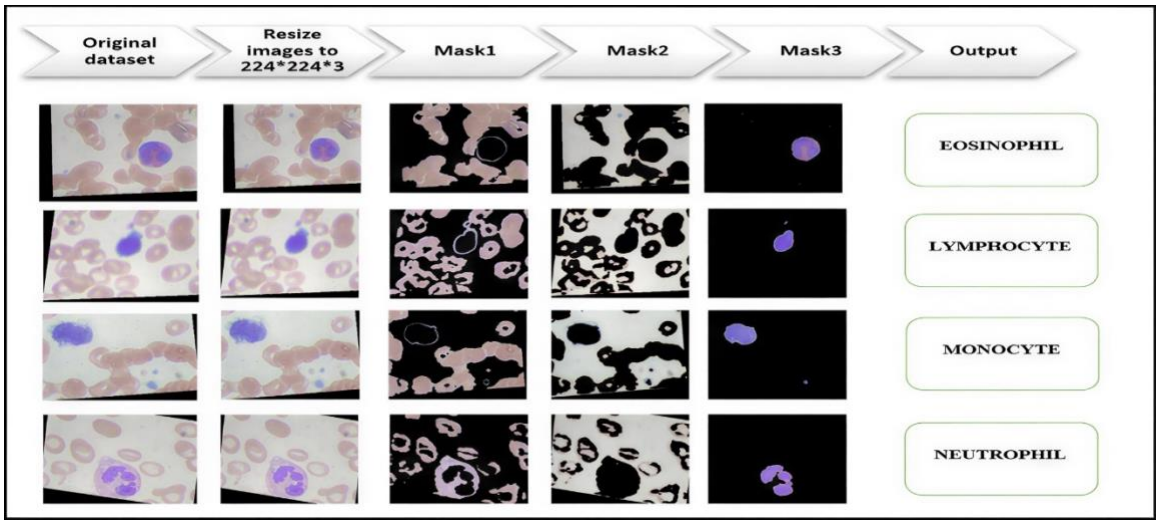

Figure 5: Overview of second experiment processing

3.5 Morphological Structuring [18]

Morphological processes are used in the process of image segmentation. Image segmentation is the discovery of some parts in a certain image that could reflect or denote meaningful aspects of the object. Filling small holes in objects, overlapping objects separation and attaching broken boundaries into connected segments are common examples of morphological factors. Meanwhile, the example of morphological processes are expansions and wears. The pixels on the border of an object are removed by erosion while stretching adds pixels to the borders of an image. This rule confirms what powers the pixels.

Dilation: Dilation represents the maximum value of the pixels in the input pixel's neighbourhood that is equal to the output value. As shown in Figure 6, the output pixel is set to a value of 1, corresponding to the pixel value in the binary image.

Similarly, Erosion: The minimum value of all the pixels in the input pixel's neighbourhood is equal to the output pixel's value. As shown in Figure 6, the output pixel is set to 0, corresponding to the pixel value in the binary image.

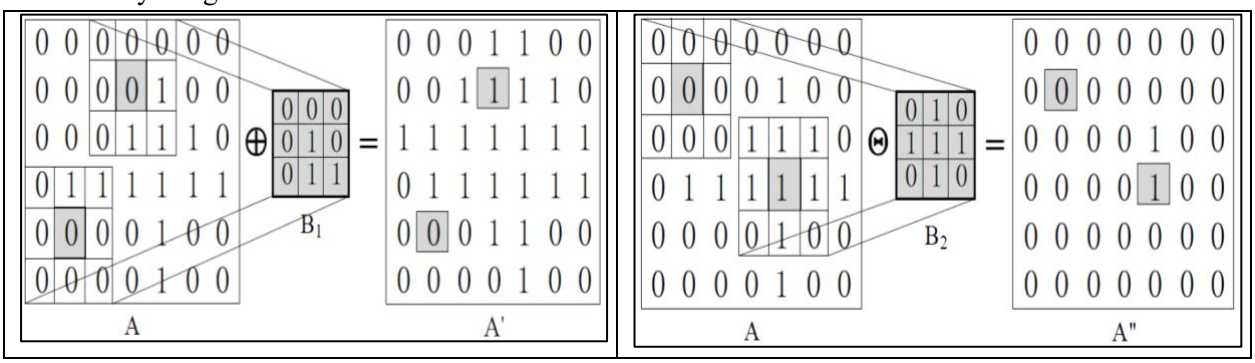

Morphological dilation	Morphological erosion

Figure 6: Morphological dilation and erosion of binary image A using structuring element B_1 and B2.

As illustrated in Figure 7, the kind of morphological operation we used in our investigation is erosion [18] with a 7×7 structuring element in the type desk. In addition, flat 2D structures are typically much smaller than the image that has been processed. A high-performance language in technical computing that is designed for programs is called MATLAB. It is used as a segmentation method [19-21].

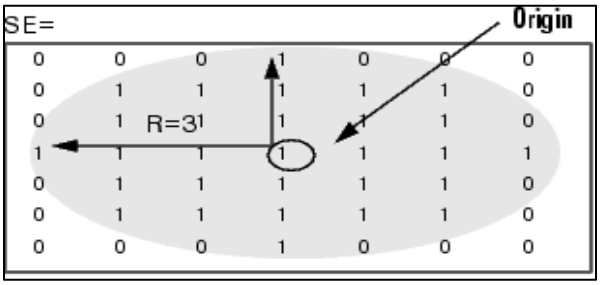

Figure 7: Morphology structuring element (desk).

A matlab function "STREL" produces the morphological structuring element. The syntax of SE (structural element) is given by Eq. (1).

$$SE = strel\,(Desk, 7) \tag{1}$$

3.6 Clustering Color

In this study, the purpose of the clustering step is to separate each blood smear image into its fundamental red (R), green (G), and blue (B) color components so that the deep learning model can learn color-specific features more effectively given in Figure 8. In blood smear images, diagnostically important structures such as the cell nucleus, cytoplasm, and surrounding background often exhibit different color distributions due to staining. These differences may not always be fully exploited when the original RGB image is used directly as input. Therefore, the proposed strategy aims to highlight the contribution of each color channel independently and generate additional informative training samples.

To achieve this, the pixel intensities of the image are analyzed in the RGB color space, where each pixel is represented by its color values. A clustering procedure, conceptually similar to k-means, is employed to group pixels according to their color similarity, which helps distinguish the dominant color information associated with the blood cell structures. After this step, the image is separated into three monochrome channel images corresponding to R, G, and B. These channel-specific images emphasize different visual characteristics of the WBC components. For example, one channel may better highlight the nucleus, while another may better preserve cytoplasmic or background details. As a result, the generated channel images provide complementary representations of the same cell.

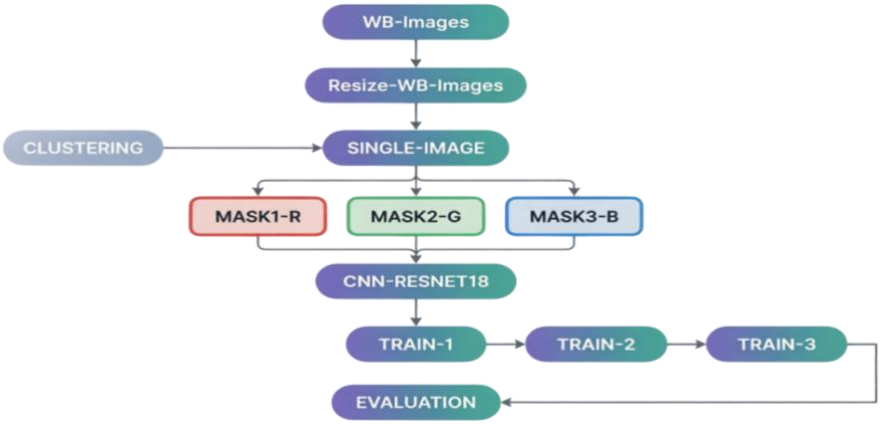

Figure 8: experiment (2) - Training ResNet-18 on the original dataset.

The main goal of this process is not clustering for segmentation alone, but rather decomposing the image into color-informed representations that can improve feature learning. By using the separated RGB channel images as part of an augmented dataset, the ResNet-18 model is exposed to richer color-sensitive information, which can improve its ability to discriminate among eosinophils, lymphocytes, monocytes, and neutrophils.

3.7 Transfer Learning

The CNN model of the suggested classifier uses transfer learning to improve learning efficacy [22-24]. The practice of applying and reusing information gained while solving one issue to another is known as transfer learning. To implement transfer learning, two things need to be made:

1. A set of layers forming the network architecture, developed by modifying a pre-existing model such as ResNet-18.
2. A labeled dataset (WB images) used for training purposes, primarily synthesized from the data repository.

Both components are provided as inputs to the network training function, which outputs the trained model.

4. Experimental Results

This section presents the results of training the low-complexity and lightweight CNN model, ResNet-18. The datasets described in [24] are used in this study. Two experiments are conducted to evaluate the model's performance. In the first experiment, the proposed classifier, there are 3091 for each category and the total number of data sets is 12364 extracted from the training data set, where each category derives about 9891 WB images and 2473 for the test step beside 64 minimum batch size. The low-complexity CNN model processes the images, a total of 20 epochs are trained twice every 10 periods. In other words, each data set is processed 20 times resulting in a total of 278 and 3100 iterations per epoch. A low-complexity CNN model processes the images, and a total of 20 epochs are trained twice every 10 periods, indicating each data set is processed 20 times. Thus, a total of 464 iterations and about 9280 iterations for each epoch is achieved, see Eq. (2) and (3), respectively.

$$Iterations\ per\ epoch\ =\ (Num.of\ samples\ /\ MiniBatchSize) \qquad (2)$$

$$Maximum\ Iterations\ =\ (Iterations\ per\ epoch * Epoch) \quad (3)$$

And the performance details of the results for experiment (1) and experiment (2) are shown in Table 1.

Table 1: Comparison between the results of the experiment (1) and experiment (2).

Performance Details	EXperiment-1	EXperiment-2
Receiver Operating Characteristic (Roc)	95.11 %	95.23 %
Training accuracy	86.89 %	**99.17** %
Epoch	20	20
Time	68 Min	74 Min
Minimum Batch Size	64	64

Here is a clearer and more polished version of your paragraph: Furthermore, during the training of Experiments-1 and Experiments-2, the accuracy and loss curves are illustrated in Figures 9 and 10. As the number of epochs increases, the accuracy steadily improves until it reaches a saturation point, where the error becomes minimal and fluctuates within a narrow range. Meanwhile, the loss gradually decreases over time and eventually stabilizes at a low value. In simple terms, accuracy reflects the model's predictive strength, whereas loss indicates the magnitude of its errors. A well-performing model is therefore characterized by high accuracy and low loss.

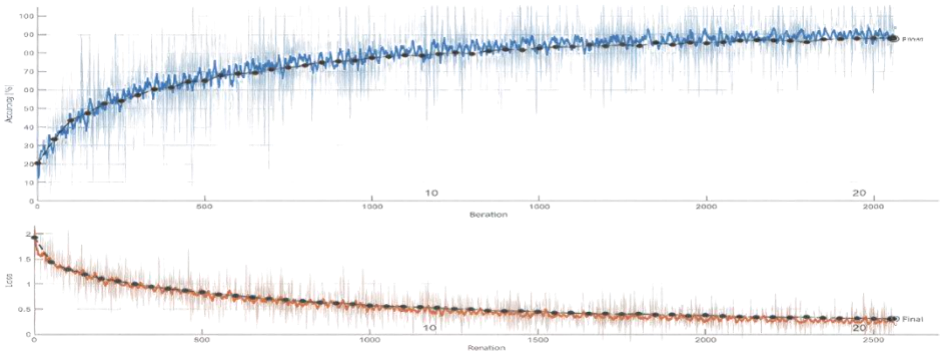

Figure 9: Training accuracy and loss curves for the original dataset (Experiment -1).

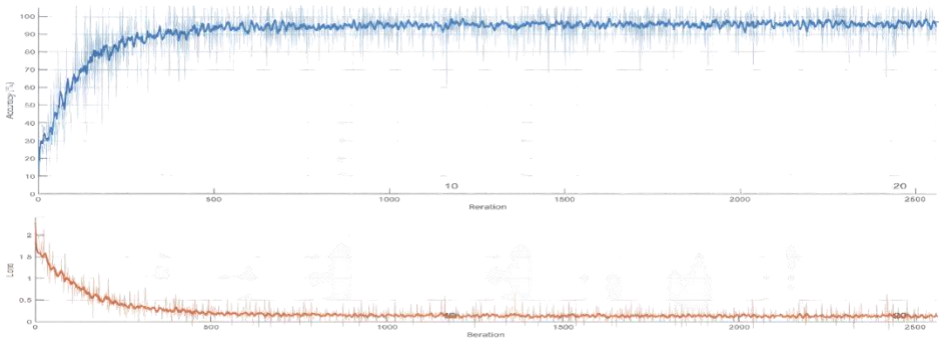

Figure 10: Training accuracy and loss curves for the new dataset (Experiment -2).

During the validation phase, the model predicts the two classes defined in the supervised learning task. The results are presented using a confusion matrix for the proposed model, where each column corresponds to the predicted classes and each row represents the actual classes. The confusion matrices for the first and second experiments are shown in Figure 11.

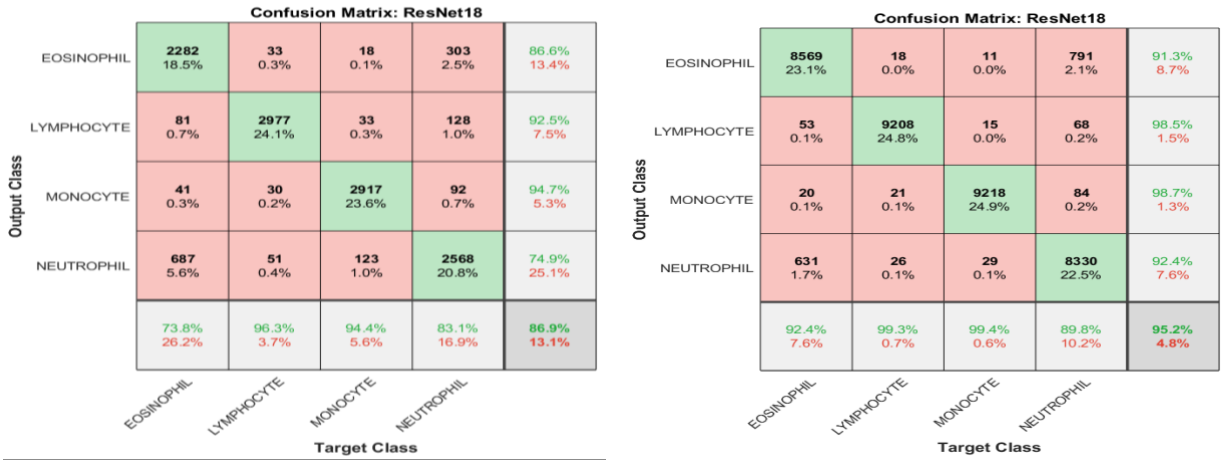

Experiment 1 **Experiment 2**

Figure 11: A confusion matrix experiment 1 and experiment 2.

In this study, accuracy, sensitivity, specificity, and precision were utilized as the performance measures, which are the most widely used metrics. The formula for computing these performance measures is shown below in Eq. (4) to 8 5 and Tables 2 and 3, respectively [25, 26], as follows:

$$\text{Accuracy} = \frac{T\,N\ +\ T\,P}{T\,P\ +\ F\,P\ +\ T\,N\ +\ F\,N} \tag{4}$$

$$\text{Sensitivity} = \frac{T\,P}{T\,P +\ F\,N} \tag{5}$$

$$\text{Specificity} = \frac{T\,N}{T\,N +\ F\,P} \tag{6}$$

$$\text{Precision} = \frac{TP}{TP + FP} \tag{7}$$

$$F\_measure = \frac{2\ (precision * sensitivity)}{precision\ +\ sensitivity} \tag{8}$$

Where, True positive (TP), False-positive (FP), True-negative (TN) and False-negative (FN).

Table 2: Findings on the performance measures of the first experiment

F- measure	Precision	Specificity	Sensitivity	Accuracy	Class
0.80	0.87	0.96	0.74	0.90	Eosinophil
0.94	0.92	0.97	0.96	0.97	Lymphocyte
0.95	0.95	0.98	0.94	0.97	Monocyte
0.79	0.75	0.90	0.83	0.89	Neutrophil

Table 3: Results of performance measures of the experiment – 2

F_ measure	Precision	Specificity	Sensitivity	Accuracy	Class
0.80	0.87	0.96	0.74	0.90	Eosinophil
0.94	0.92	0.97	0.96	0.97	Lymphocyte
0.95	0.95	0.98	0.94	0.97	Monocyte
0.79	0.75	0.90	0.83	0.89	Neutrophil

5. Conclusion

Developed a deep learning approach to classify WB images, classify eosinophils, lymphocytes, Monocytes and Neutrophil Cells, based on a novel strategy for assembling RGB channels of a blood sample image using the Resnet-18 Model. Using image enhancement technology as a preprocessing step improves classification accuracy. The results validated the comparison in two experiments, with no improvement on datasets that achieved an overall accuracy of 86.89% and after utilizing an image-optimization and clustering process where the performance was 99.17% higher. Based on the aforementioned results, this study concludes that the data processing assisted in enhancing the rate of the classification output. Future works can include more approved datasets from WHO to develop a novel convolutional neural network. Furthermore, doctors and medical practitioners may be assisted by creating an integrated system that will enable them to determine the population and types of WBCs. This could be achieved by employing some engineering devices by cropping vital aspects of images or using filters to minimise the time taken to execute data analysis.

Funding Statement: The author(s) received no specific funding for this study.

Data Availability: The data that support the findings of this study are reported in Section 3.1 of this article.

Conflicts of Interest: The authors declare no conflicts of interest regarding this study.

Authors contributions. Conceptualization: AA, DK,; data curation and methodology : AA, AS; validation and visulization: AA, SA, AS; writing—original draft preparation: AA, DK, SA, AS; writing—review and editing: DK, SA, AS; supervision and project administration: SA, AS. All authors had approved the final version.

References

[1] Baghel, N., Verma, U. and Nagwanshi, K.K., (2022). "WBCs-Net: Type identification of white blood cells using convolutional neural network". *Multimedia tools and applications*, 81(29), 42131-42147.

[2] Herron, C., (2012). "Know your wbcs". *Nursing Made Incredibly Easy*, 10(1), 11-15.

[3] Thachil, J., (2021). "Are white blood cells white? ". *British Journal of Haematology*, 193(4).

[4] Hu, S., Yu, B., Xu, R. et al., (2025). "Leukocyte analysis: Current status and future direction". *Clinica Chimica Acta*, 120477.

[5] Muller, W.A., (2013). "Getting leukocytes to the site of inflammation". *Veterinary pathology*, 50(1), 7-22.

[6] Szelenyi, I., (2007). "Overview on the immune response". *Planta Medica*, 73(09), WS_5_01.

[7] BRINK, (1998). "Gap junctions in vascular smooth muscle". *Acta physiologica scandinavica*, 164(4), 349-356.

[8] Armstrong, C.E. and Mason, L., (2025). "Physiology of red and white blood cells". *Anaesthesia & Intensive Care Medicine*, 26(1), 48-52.

[9] Jung, C., Abuhamad, M., Mohaisen, D., et al., (2022). "WBC image classification and generative models based on convolutional neural network". *BMC Medical Imaging*, 22(1), 94.

[10] Manley, H.R., Keightley, M.C. and Lieschke, G.J., (2018). "The neutrophil nucleus: an important influence on neutrophil migration and function". *Frontiers in immunology*, 9, 2867.

[11] Ondari, E., Calvino-Sanles, E., First, N.J, et al., (2021). "Eosinophils and bacteria, the beginning of a story". *International journal of molecular sciences*, *22*(15), 8004.

[12] Shah, H., Eisenbarth, S., Tormey, C.A. et al., (2021). "Behind the scenes with basophils: an emerging therapeutic target". *Immunotherapy advances*, 1(1), p.ltab008.

[13] Alabdulkreem, E., Elmannai, H., Saad, A., et al., (2024). "Deep Learning-Based Classification of Melanoma and Non-Melanoma Skin Cancer". *Traitement du Signal*, 41(1).

[14] Geissmann, F., Manz, M.G., Jung, S., et al., (2010). "Development of monocytes, macrophages, and dendritic cells". *Science*, *327*(5966), 656-661.

[15] Ali, C.J. and Ahmed, M.A., (2018). "Evaluation of hematocrit level, red blood cells and white blood cells counts in blood from patients with different severities of periodontal diseases".

[16] A. Rahman., "WBC multiclass dataset). [Online]. Available, https://www.kaggle.com/alifrahman/main-dataset.

[17] Shafiq, M. and Gu, Z., (2022). "Deep residual learning for image recognition: A survey". *Applied sciences*, 12(18), 8972.

[18] Gan, Z., Guo, S., Chen, C., et al., (2024). "Tracking the 2D/3D morphological changes of tidal flats using time series remote sensing data in Northern China". *Remote Sensing*, 16(5), 886.

[19] Ijemaru, G. and Nwajana, A., (2021). "Image processing system using MATLAB-based analytics". *Bulletin of Electrical Engineering and Informatics*, 10(5), pp.2566-2577.

[20] Abdulrahman, A. and Varol, S., (2020). "A Review of Image Segmentation Using MATLAB Environment". *ISDFS*, 1-5.

[21] Al-Ameen, Z., Muttar, A. and Al-Badrani, G., (2019). "Improving the Sharpness of Digital Image Using an Amended Unsharp Mask Filter". *International Journal of Image, Graphics & Signal Processing*, 11(3).

[22] Magotra, A. and Kim, J., (2019). "Transfer learning for image classification using hebbian plasticity principles". In *Proceedings of the 2019 3rd International Conference on Computer Science and Artificial Intelligence*, 233-238.

[23] Zhuang, F., Qi, Z., Duan, K., et al., (2020). "A comprehensive survey on transfer learning". *Proceedings of the IEEE*, 109(1), 43-76.

[24] Yang, F., Zhang, W., Tao, L. et al., (2020). "Transfer learning strategies for deep learning-based PHM algorithms". *Applied Sciences*, *10*(7), p.2361.

[25] Hadjouni, M., Elmannai, H., Saad, A., et al., (2023). "A novel deep learning approach for brain tumors classification using MRI images". *Traitement du Signal*, 40(3).

[26] Elaraby, A., Saad, A., Karamti, H. et al., (2023). "An Optimized Deep Learning Approach for Robust Image Quality Classification". *Traitement du Signal*, 40(4), 1573.